# T-437 Asymmetry Results

**November 2, 2001**

*B. Humensky*

## Introduction

This note summarizes beam conditions and asymmetry measurements during T-437, a beam test for E158 that ran from Nov 1-8, 2000. The key goals of the test were to commission the polarized source for high-current running in the Spring of 2001, to demonstrate control over helicity-correlated beam charge and position asymmetries, and to demonstrate toroid and cavity BPM resolution and agreement at an improved level over Gun Test Lab and ASSET99 studies. Table 1 summarizes the goals for charge and position asymmetries and puts them into perspective relative to past performance and what is required for the physics runs. The goals for T-437 were determined by what statistics can be reasonably achieved in a week's running time. Comparing the second and last columns of table 1, we see the results achieved are so far limited only by the statistics we were actually able to acquire and come close to the stated goals.

Two results are quoted for the intensity asymmetry and for the X and Y position differences, a $1/\sqrt{N}$ value and a 1/N value. The $1/\sqrt{N}$ value is an weighted average over the appropriate runs with the weight being determined in the orthodox manner: using the error bar for each run, where the error is the RMS/$\sqrt{N}$, with N the number of pulses in the run. The 1/N values are calculated slightly differently, and are meant to indicate how well the intensity asymmetry and position difference feedbacks succeed at achieving the superstatistical scaling they are capable of. The means are calculated by weighting the individual runs that enter into the averages by their 1/N errors, which assumes perfect 1/N scaling on each feedback run. However, this weighting, even if 1/N scaling is perfect, does not accurately reflect the statistical weight of the runs, which should be proportional to the number of electrons in the run, and hence fairly close to the error bar given by calculating RMS/$\sqrt{N}$. These means are included to be consistent with the results presented at the collaboration meeting of Nov 17, 2000, but probably should not be given much weight. The interesting feature is to compare the $1/\sqrt{N}$ means with their errors and with the 1/N errors. The former demonstrates that our results are consistent with zero, and the latter gives an indication of how well the feedbacks are working.

The next section will describe the experimental setup, and the following sections will describe results for studies under various conditions. The last section draws conclusions and summarizes open questions. An appendix includes tables of results from individual runs.

## Setup

The polarized source provided a 59Hz beam with 1Hz of pedestal. The beam pulse was $2.3 * 10^{11}$ electrons in 370ns. We expect that the beam had roughly 70% polarization with

| | Achieved in GTL | T-437 Goal | E158 Goal | T-437 Achieved |
|---|---|---|---|---|
| Intensity Asymmetry | $2 . 10^{-7}$ | $2 . 10^{-7}$ | $2 . 10^{-7}$ | 2.22 $\pm$56.53 $. 10^{-7}$ $1/\sqrt{N}$<br>0.76 $\pm$3.34 $. 10^{-7}$ 1/N |
| Toroid Asymmetry Agreement | $10^{-6}$ | $10^{-8}$ | $10^{-9}$ | $0.6 \pm 1.2 . 10^{-8}$ |
| X Position Difference | 5nm | 10nm | 10nm | -6 $\pm$ 37 nm $1/\sqrt{N}$<br>-8 $\pm$6 nm 1/N |
| Y Position Difference | 5nm | 10nm | 10nm | -19 $\pm$ 49 nm $1/\sqrt{N}$<br>-17 $\pm$8 nm 1/N |
| BPM Difference Agreement | 100nm | 1nm | 1nm | $X : -1.4 \pm 0.9$ nm<br>$Y : -4.2 \pm 1.8$ nm |

Table 1: Goals for T-437. Results in last column limited by actual statistics acquired.

the laser wavelength set at 854nm, but this was not measured. The beam was dumped at 2-9 with an energy of 1.2GeV.

Beam monitoring devices are located in two areas and read out by two separate DAQs. Devices in the Injector region are read out by SCP–the SLC Control Program. They include three BPMs: 392 and 402 between the PGUN and the first bending magnet, and 405 downstream of the bending magnet. There are also two toroids: 488 and 560, both located downstream of the first accelerating section, where the beam is at 40MeV. BPM 392 can be used in a helicity-correlated position difference feedback loop, and toroid 488 can be used in a helicity-correlated intensity asymmetry feedback loop. BPM 392 was not reading out properly until the morning of Nov 6th.

Devices in the ASSET region are read out by the E158 DAQ. They include 3 cavity BPMs named A1, A2, and B, and two toroids: T1 and T2. Any of the BPMs or toroids can be used as measuring devices in the relevant feedback loops. The ASSET data is logged to disk from the online "anal" program, and to tape using the "control" program. Slow monitor information, typically read out by MCCSTAT, is not recorded for this run. Intensity feedback miniruns are 2000 pulse pairs long; position feedback miniruns are 10K pulse pairs long.

The control devices for the intensity and position feedbacks are located on the Wall Bench in the CID Laser Room. They are described in a separate document "E158 Source Optics."

## Toroid Agreement and Charge Asymmetries

One goal for T-437 was to demonstrate that two toroids could measure the same charge asymmetry at the $10^{-8}$ level. Table 2 shows our results on the difference in asymmetry for runs of various types. The typical intensity asymmetries during these runs were at the level of 1-2$.10^{-5}$. During all runs but the E158 Feedback runs, the SCP Intensity Asymmetry feedback was running in the injector. The SCP feedback zeroed the asymmetry at one injector toroid, but showed disagreement at the second toroid at the 20ppm level; this level of residual asymmetry also shows up at ASSET. Overall, the result is consistent with zero with a 12ppb statistical error, so our ability to demonstrate toroid agreement is so far statistics-limited.

A second goal was to demonstrate that with the intensity asymmetry feedback we could achieve an integrated asymmetry below 100ppb. Table 3 summarizes the results of the E158 FDBK runs for the asymmetry on the individual toroids. Again, the result is simply statistics-limited.

Figures 2, 5, and 6 in the Appendix include the run-by-run results for each ASSET toroid for the various runs involved in these summary tables.

| Class of Runs | A1 - A2 (ppb) |
|---|---|
| $\lambda/2$ IN | -31 $\pm$ 25 |
| $\lambda/2$ OUT | -27 $\pm$ 24 |
| E158 FDBKS ($\lambda/2$ OUT) | 13 $\pm$ 24 |
| Other Runs ($\lambda/2$ OUT) | -33 $\pm$ 23 |
| AVERAGE | -20 $\pm$ 12 |
| AVERAGE sign flip | 6 $\pm$ 12 |

Table 2: Probing agreement between the two toroids. 'A1' is the intensity asymmetry measured by Toroid 1; 'A2' is the intensity asymmetry measured by Toroid 2. The goal was to reach an error of 10ppb. The measurement was statistics-limited. For detailed results of each run, see figures 2,5,6 in the Appendix.

| | $1/\sqrt{N}$ scaling | 1/N scaling |
|---|---|---|
| Toroid 1 | 0.22 $\pm$ 5.65 ppm | 76 $\pm$ 334 ppb |
| Toroid 2 | 0.16 $\pm$ 5.65 ppm | -15 $\pm$ 333 ppb |

Table 3: Charge Asymmetry. Using feedback on Toroid 1 to drive charge asymmetry to zero. For detailed results of the runs involved, see figure 5 in the Appendix.

## Position Differences and BPM Agreement

Table 4 summarizes results on the quality of agreement in the measurement of position differences between the cavity BPMs at ASSET. The algorithm to determine agreement is to use the measurements at the first and last BPMs to predict what the position differences should be at the second BPM, and then compare that prediction with what is actually measured on a pulse-by-pulse basis. This algorithm removes noise associated with the beam itself, which will be common to all three BPMs, and leaves (for the most part) only the noise associated with the BPM readout electronics. The numbers quoted in the table are the differences between the predicted and measured values at the second BPM. This analysis also tells us the resolution with which the BPMs measure the beam position, and with fairly minimal massaging of the data, we were able to achieve resolutions as low as 900nm for the

X position and 2-3$\mu$m for the Y position. Presumably, with more work on the beam tune and data processing, we'll be able to bring the Y position resolution down to the 1$\mu$m level.

Several types of runs are tabulated in table 4. The first two rows, $\lambda/2$ IN and OUT, refer to a set of studies in which, without running the position feedback, we ran while alternating the state of the insertable half-wave plate every two hours. As described in the following section, in averaging these data sets we anticipate a sign flip in the physics asymmetry, allowing us to flip the sign of one data set before averaging. This results in a significant degree of cancellation of systematics. The fourth row, E158 FDBKS, refers to a set of runs for which both the intensity asymmetry and position difference feedbacks were operating under E158 control, and for these runs the measured asymmetries on each individual device were also consistent with zero at the level of statistics. The Grand AVG is a weighted average of the third and fourth lines.

The X agreement is good to a few nm on the individual types of runs, in the presence of position differences of a couple hundred nm. The Y disagreement for $\lambda/2$ IN runs is about 22nm in the presence of roughly 1.5-2.0$\mu$m position differences; the Y disagreement for $\lambda/2$ OUT runs is about 10nm in the presence of roughly 0.5-1.0$\mu$m position differences. So it looks like there may be a rough scaling of BPM agreement with the size of the position differences, with something like agreement at a level of approximately 1-2% of the position differences. It is also interesting that the BPM agreement shows a fair bit of cancellation between the $\lambda/2$ IN and OUT states, comparable to the cancellation we see between the position differences. Approximately 1.8 million pairs of measurements are present in the grand average. See figures 3,4,7, and 8 in the Appendix for the detailed run-by-run results.

| Class of Runs | X Agree (nm) | Y Agree (nm) |
|---|---|---|
| $\lambda/2$ IN | -3.1 $\pm$ 1.4 | 21.5 $\pm$ 3.7 |
| $\lambda/2$ OUT | -4.6 $\pm$ 1.3 | 9.7 $\pm$ 3.4 |
| AVG Sign Flip | -1.1 $\pm$ 0.9 | -4.4 $\pm$ 2.5 |
| E158 FDBKS | -3.6 $\pm$ 2.5 | -4.0 $\pm$ 2.5 |
| | | |
| Grand AVG | -1.4 $\pm$ 0.9 | -4.2 $\pm$ 1.8 |

Table 4: BPM Agreement. X and Y position differences are taken to be at the middle ASSET BPM. X and Y angle differences are calculated from the change in position difference between the first and last ASSET BPMs over the two meter separation between them. See figures 3,4,7,8 in the Appendix for detailed run-by-run results.

Table 5 summarizes results from E158 position loop feedback runs. We only had two such runs, one in each state of the Asymmetry Inverter, and the results of the individual runs are compared in a later section. It should be noted that the Asymmetry Inverter provides some degree of cancellation of position systematics. However, we did see that during each run, each of the three BPM's integrated position differences were converging to zero with close to 1/N scaling. Figure 1 shows the Y position differences converging to zero for one of the runs, and is typical of the quality of convergence we see with the position feedback. The two runs totalled roughly 700 thousand pairs of measurements. Results are presented with averaging assuming both 1/N scaling and $1/\sqrt{N}$ scaling of the errors. Ie, the weighting of the results for each run in the average was done assuming both statistical scaling and perfect 1/N scaling. The validity of weighting by the 1/N errors is uncertain, but it gives a useful guide to the quality of the position difference feedback's performance. Again, the mean values for the $1/sqrt(N)$ are the ones to pay attention to. It is encouraging to see the results consistent with zero at the level of our statistics. See figures 7 and 8 in the Appendix for the detailed results of these runs.

| | 1/N errors | $1/\sqrt{N}$ errors |
|---|---|---|
| X pos | -8 ± 6 nm | -6 ± 37 nm |
| X angle | 5 ± 5 nrad | 8 ± 31 nrad |
| Y pos | -17 ± 8 nm | -19 ± 49 nm |
| Y angle | -12 ± 6 nrad | -11 ± 34 nrad |

Table 5: Position Differences. X and Y position differences are taken to be at the middle ASSET BPM. X and Y angle differences are calculated from the change in position difference between the first and last ASSET BPMs over the two meter separation between them. See figures 7 and 8 in the Appendix for the detailed results of these runs.

## Inversions I: Half-Wave Plate

The idea behind inserting a half-wave plate into the laser beam at the source is that it will invert the laser light helicity, providing a flip of the definition of the electron beam helicity. Ideally this will flip the sign of the physics asymmetry without changing any false asymmetries, providing a means of cancelling false asymmetries by running for equal time in the two states. The results summarized in Table 6 were taken while running the Intensity Asymmetry feedback under SCP control on Injector Toroid 488 while measuring with the ASSET BPMs and Toroids. The data was taken overnight, over approximately a 12-hour period, and considerable drifts in the position differences were in evidence. Still, we see some cancellation of position, angle, and charge effects. There was no position feedback running at this time. Figures 2, 3, and 4 in the appendix include the run-by-run results for each toroid and BPM at ASSET during the half-wave cancellation studies.

The results in Table 7 show that the position systematics are very sensitive to the insertion of a half-wave plate on the CID Gun Bench. Note that for this set of runs, we did not adjust the CP or PS cell voltages when inserting the half-wave plate, causing the IA loop to make a 0.3% correction with the half-wave plate IN versus $< 0.05\%$ with the half-wave plate OUT.

Table 8 contains additional half-wave plate cancellation data, but this time with the half-wave plate inserted the PS cell voltages were adjusted to null the intensity asymmetry, keeping the IA loop corrections down to the few $10^{-4}$ level. Comparing the half-wave plate IN data between tables 7 and 8, the failure to null the intensity asymmetry by adjusting the CP and PS cell voltages does not appear to make a change in the position systematics

| Asymmetry | $\lambda/2$ IN | $\lambda/2$ OUT | AVG |
|---|---|---|---|
| X Position | 126 ± 12 nm | 119 ± 11 nm | -7 ± 8 nm |
| X Angle | -25 ± 10 nrad | -105 ± 10 nrad | 43 ± 7 nrad |
| Y Position | -1732 ± 57 nm | -581 ± 51 nm | -461 ± 38 nm |
| Y Angle | -24 ± 41 nrad | -32 ± 38 nrad | 8 ± 28 nrad |
| Toroid 1 | -1.5 ± 5.1 ppm | -14.7 ± 4.7 ppm | 7.2 ± 3.5 ppm |

Table 6: Half-wave plate inversion results. X and Y position differences are taken to be at the middle ASSET BPM. X and Y angle differences are calculated from the change in position difference between the first and last ASSET BPMs over the two meter separation between them. Figures 2,3,4 in the Appendix contain the detailed run-by-run results.

| Meas | 1005 | 1007 | 1008 | 1009 |
|---|---|---|---|---|
| TR488 (ppm) | -2.5 ± 26/1.5 | | | |
| TR560 (ppm) | -28 ± 25/1.5 | | | |
| X402 (nm) | 3550 ± 175 | -4000 ± 940 | 3000 ± 880 | -4000 ± 840 |
| Y402 (nm) | -430 ± 157 | -6000 ± 760 | -1000 ± 710 | -5000 ± 680 |
| X405 (nm) | 140 ± 241 | | | |
| Y405 (nm) | 700 ± 341 | | | |
| IA corr (ppm) | 250 ± 56 | -3300 ± 409 | 500 ± 374 | -3300 ± 366 |
| # runs | ˜ 275 | | | |
| Notes | $\lambda/2$ OUT<br>dCP, dPS at nominal all runs | $\lambda/2$ IN | $\lambda/2$ OUT | $\lambda/2$ IN |

Table 7: SCP DAQ Results Overnight, toggling $\lambda/2$ plate but not touching CP or PS voltages; with $\lambda/2$ IN, SCP IA loop has to make a large correction. Position loop in compute.

at a level significant with respect to the error bars of these runs, typically on the order of 500-900nm.

| Meas | 1013 | 1014 | 1015 | 1016 | 1017 | 1018 |
|---|---|---|---|---|---|---|
| T488 ppm | 0 $\pm$ 28/2 | | | | | |
| T560 ppm | -21 $\pm$ 28/2 | | | | | |
| X402 ($\mu$m) | 3.2 $\pm$ .164 | -4.5 $\pm$ .5 | 2.7 $\pm$ .5 | -3.5 $\pm$ .5 | 3.0 $\pm$ .5 | -4.2 $\pm$ .5 |
| Y402 ($\mu$m) | -.13 $\pm$ .276 | -5.5 $\pm$ .85 | -2.4 $\pm$ .85 | -5.5 $\pm$ .85 | -1.3 $\pm$ .85 | -5.0 $\pm$ .85 |
| IAcor ppm | -33 $\pm$ 61 | 0 $\pm$ 67 | 200 $\pm$ 56 | 250 $\pm$ 64 | 0 $\pm$ 59 | 250 $\pm$ 64 |
| # runs | | | | | | ~158 |
| Notes | dPS=0 $\lambda/2$ OUT | dPS=-44 $\lambda/2$ IN | dPS=0 $\lambda/2$ OUT | dPS=-44 $\lambda/2$ IN | dPS=0 $\lambda/2$ OUT | dPS=-44 $\lambda/2$ IN |

Table 8: SCP DAQ Results Overnight, toggling $\lambda/2$ plate and nulling intensity asymmetry with PS cell voltage. SCP Intensity feedback running, position loop in compute.

## Inversions II: Asymmetry Inverter

The Asymmetry Inverter is two sets of lenses on a translation stage. One set puts a +2I transformation on the laser beam; the other a -2I transformation. This provides a means of inverting the spatial profile, position and angle, of the laser beam as it hits the cathode and should invert any position systematics generated upstream of it. The data in Table 9 were taken while running the Intensity Asymmetry feedback under E158 control on Toroid 1 at ASSET, and the Position Difference feedback under E158 control on BPM A2 (the middle BPM). Also running with $\Delta$CP = +400V. We see a nice cancellation of the (large) Y position difference. Comparing this data with the E158 FDBKs line of table 4, we see that while Y requires a correction on the order of $1\mu$, the BPM agreement is still at the level of a few nm, suggesting that along with feedback driving the position differences down by two orders of magnitude, it also maintains a level of BPM agreement greater than two orders of magnitude better than the size of the corrections.

The data in Table 10 are results from the Injector diagnostics. We did not begin recording +2I data until about 1 hour into the run, which was just under 3 hours long total. The -2I run was 4.33 hours long. I think we would expect to see these asymmetries roughly the same for the two runs: we're driving the ASSET position differences to zero, and some position difference at the Injector transforms to zero at ASSET. So I'd expect that to get zero at ASSET we'd have to have a particular value in the Injector, regardless of the choice of optics state upstream.

Also see the data on the individual ASSET BPMs in the tables in Figures 7 and 8.

| Fdbk Induced Asym | -2I State | +2I State | AVG |
|---|---|---|---|
| X Position | 262 ± 48 nm | -39 ± 71 nm | 168 ± 40 nm |
| Y Position | -862 ± 109 nm | 1157 ± 130 nm | -29 ± 84 nm |
| Toroid 1 | -281 ± 20 ppm | 78 ± 29 ppm | -165 ± 16 ppm |

Table 9: Asymmetry Inverter results. X and Y position differences are taken to be at the middle ASSET BPM. X and Y angle differences are calculated from the change in position difference between the first and last ASSET BPMs over the two meter separation between them. Figures 5,7,8 in the Appendix contain the detailed run-by-run results.

| Asymmetry | -2I State | +2I State |
|---|---|---|
| Tor488 | 22 ± 29 ppm | 0 ± 47 ppm |
| Tor560 | 8 ± 29 ppm | -12 ± 49 ppm |
| X392 | -250 ± 234 nm | -1300 ± 485 nm |
| X402 | 1500 ± 234 nm | 200 ± 569 nm |
| X405 | 350 ± 250 nm | -250 ± 467 nm |
| Y392 | -2800 ± 178 nm | -1350 ± 286 nm |
| Y402 | -4600 ± 226 nm | -4150 ± 374 nm |
| Y405 | 225 ± 408 nm | -200 ± 617 nm |
| # Runs | 415 | 157 |

Table 10: SCP/Injector Results with Asymmetry Inverter

## Sensitivity to ΔCP and ΔPS Voltages

Table 11 summarizes the sensitivity to the ΔCP and ΔPS voltages chosen. At ASSET, there is only appreciable sensitivity to Y position, and even then the sensitivity is not that large. For most of the test we ran at a ΔCP of +400V in an effort to bring down the Y position difference, but that is a larger ΔCP than we'd typically feel comfortable making. We'd prefer to set a limit of something like ΔCP $< \pm 200V$. The physical origin of this sensitivity is not well understood, but likely arises from some sort of spatial variation on the cathode of its sensitivity to the quantity of linear polarization striking it.

Table 12 shows how systematics measured in the Injector BPMs and toroids vary with ΔCP and ΔPS voltages, ie. as we slide the Pockels cell voltages along the Qasym=0 line. The only sensitivity of note is BPM402Y, which shows a reasonably-sized slope. Unfortunately, comparing these results with those for the ASSET BPMs, we find that making the ASSET Y position differences smaller makes the BPM402Y Position differences larger. The implication would seem to be that something is changing the systematics downstream of the Injector BPMs, perhaps due to clipping of the beam as it leaves the Injector region.

| Change in... | as $\Delta$CP changes |
|---|---|
| X Position | 0.03 $\pm$ 0.03 nm/V |
| X Angle | -0.01 $\pm$ 0.02 nrad/V |
| Y Position | 1.17 $\pm$ 0.19 nm/V |
| Y Angle | -0.04 $\pm$ 0.15 nrad/V |
| X402 Pos | 3.611 $\pm$ 0.292 nm/V |
| $\Delta$PS | -0.346 $\pm$ 0.007 V/V |

Table 11: Sensitivity to location along Charge Asymmetry = 0 line in voltage space, as a function of $\Delta$CP voltage. Figures 7,8 in the Appendix contain the detailed run-by-run results.

| Meas | 1002-01 | 1003 | 1004 |
|---|---|---|---|
| TR488 (ppm) | -6 $\pm$ 31/3.1 | 2 $\pm$ 53 | 0.7 $\pm$ 30 |
| TR560 (ppm) | -7 $\pm$ 30/3.0 | | |
| X392 (nm) | | | |
| Y392 (nm) | | | |
| X402 (nm) | 3838 $\pm$ 124 | 1674 $\pm$ 131 | 3308 $\pm$ 140 |
| Y402 (nm) | -42 $\pm$ 205 | 271 $\pm$ 168 | 170 $\pm$ 140 |
| X405 (nm) | -693 $\pm$ 358 | -79 $\pm$ 336 | -57 $\pm$ 280 |
| Y405 (nm) | -150 $\pm$ 380 | 111 $\pm$ 341 | 76 $\pm$ 373 |
| IA corr (ppm) | | | |
| # runs | | | |
| Notes | dCP=+300 $\lambda/2$ OUT | dCP=-300 $\lambda/2$ OUT | dCP=+150 $\lambda/2$ OUT |

Table 12: SCP DAQ Results Overnight, studying sensitivity of position systematics to $\Delta$CP and $\Delta$PS voltages.

## Beam Scaling from CID to ASSET

It was expected that the electron beam diameter would drop by a factor of 10-50 between CID and ASSET. Our best indicator on beam size scaling comes from comparing the dynamic range of the position feedback in the CID and ASSET BPMs. At CID, driving the piezo mirror full-range yields position differences on the order of 60$\mu$m each in X-Tilt and Y-Tilt. At ASSET, X-Tilt yields a range of about 10$\mu$m, and Y-Tilt a range of about 25$\mu$m. This suggests a decrease in size of about a factor of 2.5 in Y and 6 in X, but the beam phase also needs to be considered: some of the sensitivity to position at the cathode has also been turned into sensitivity to angle at ASSET. We had expected that position differences would scale roughly with the size of the beam, so this study of the dynamic range of the position feedback says that either the beam size is an order of magnitude larger than expected, or position differences won't scale with spotsize from the cathode as simply as we anticipated.

## Running Conditions I: Pulse Length

Table 13 summarizes the results from a study of how systematics vary with pulse length. We shortened the pulse length by a factor of five, with a corresponding decrease in the amount of current. Short-pulse results are shown for two different cuts on the absolute position of the beam because while our normal cut is at 0.5mm, the centroid of the beam was roughly 0.5-0.6mm off-center in Y. Since the beam tune did not change between these two runs, we interpret this as the beam having a vertical tilt, such that the head of the pulse is off-center in one direction and the tail is presumably off-center in the other direction. We see that the position differences have a clear temporal dependence, while it appears the angle difference may be more constant.

| Asymmetry | 370ns, | 75ns, $< 0.5$mm | 75ns, $< 0.8$mm |
|---|---|---|---|
| X pos | -144 $\pm$ 11 nm | -260 $\pm$ 37 nm | -260 $\pm$ 37 nm |
| X angle | -40 $\pm$ 8 nrad | -64 $\pm$ 28 nrad | -64 $\pm$ 28 nrad |
| Y pos | -315 $\pm$ 54 nm | 621 $\pm$ 305 nm | 554 $\pm$ 126 nm |
| Y angle | -49 $\pm$ 43 nrad | 96 $\pm$ 253 nrad | -59 $\pm$ 96 nrad |
| Toroid 1 | -33 $\pm$ 8 ppm | -20 $\pm$ 23 ppm | |

Table 13: Dependence of Systematics on Pulse Length. Figures 6-8 in the Appendix contain the detailed run-by-run results.

## Running Conditions II: Beam Phase

Table 14 summarizes the results from a study of how systematics vary with beam phase. The "Before" run is the last run before a particular broken quad (its current would not stay stable) was turned off and the lattice retuned to work without it. The two "After" runs are the first two runs after the retuning. While there is clearly a significant difference between the "Before" and "After" runs, there is also a significant difference between the two "After" runs, another suggestion that the systematics have instabilities that are as yet not understood.

| Asymmetry | Before | After 1 | After 2 |
|---|---|---|---|
| X pos | -144 $\pm$ 11 nm | 25 $\pm$ 36 nm | -291 $\pm$ 25 nm |
| X angle | -40 $\pm$ 8 nrad | 2 $\pm$ 26 nrad | 32 $\pm$ 20 nrad |
| Y pos | -315 $\pm$ 54 nm | 30 $\pm$ 124 nm | 853 $\pm$ 60 nm |
| Y angle | -49 $\pm$ 43 nrad | 4 $\pm$ 86 nrad | 86 $\pm$ 35 nrad |
| Toroid 1 | -33 $\pm$ 8 ppm | | |

Table 14: Dependence of Systematics on Beam Phase. See figures 5-8 in the Appendix for detailed run-by-run results.

## Summary and Discussion

We came up short of demonstrating our BPM and Toroid asymmetry goals because we were limited by available statistics. However, we did demonstrate that we can achieve charge asymmetries on the order of 0.33ppm with toroid agreement on the order of 10ppb. Likewise, we demonstrated that we can use feedback to bring position differences down two orders of magnitude, from $1\mu$m to around 10nm. Simultaneously, we demonstrated BPM agreement at the level of a few nm. In addition, it looks like there's a rough scaling evident in which, without feedback, the quality of the BPM agreement may be at the level of 1-2% of the level of measured position differences. With feedback, the BPM agreement appears to be at a level significantly better than 1% of the correction applied.

Other key results include observing that position systematics are sensitive to a large number of parameters: the choice of CP and PS Pockels cell voltages, the beam phase, and the length of the beam pulse. It is important to be aware of these dependencies, but whether we can use them as knobs to control the systematics remains to be seen. The voltage dependence was too weak to provide a means of zeroing the position differences at ASSET, but it did give us a few hundred nm range. It remains to be seen how much freedom we'll have in choosing the beam phase on target. Many factors will go into determining the optimal pulse length: luminosity, target density fluctuations, losses in the spectrometer, beam loading, systematics, and more.

A number of open issues remain. First, what is the optimization procedure we should use to minimize the position differences before turning on the feedback? The knobs at our disposal include the orientation of the insertable half-wave plate, the choice of operating voltages for the CP and PS cells, and translations of the CP and PS cells relative to the laser beam. We can also choose to run either all in one particular asymmetry inverter state, or split the running between two states to take advantage of a cancellation.

Second, it was expected that the beam spotsize at ASSET would be a factor of 10-50 smaller than at the cathode, and a corresponding decrease in systematics was also expected. But what we observed was more like a factor of 3 decrease in systematics and a factor of 2.5-6 decrease in the dynamic range of the position feedback. This is a concern because we had hoped to find an order of magnitude reduction of systematics between the cathode and the target, in part from a reduction in beam size of a factor of 3-4 and in part from emittance growth in the accelerator. So it remains very interesting to see what we will measure the first time we put high-current beam through the A-Line and Alcove BPMs.

Third, a number of other issues unrelated to beam asymmetries arose that will be important for the physics run. They include

1. Dependence of laser wavelength of temperature and humidity.
2. Overhead on laser power due to cesiation cycle, temperature, and humidity.
3. Tilt plate checkout still to do.
4. Cathode charge limit–problem since solved by additional activations of the cathode; sufficient current now achievable.
5. Implementing absolute steering and intensity feedbacks.
6. Understanding and controlling the beam phase; implementing an "asymmetry inverter" in the electron beam optics.

7. Attenuation and sharing of stripline BPMS (PEP-II compatibility).

8. Electronics concerns, including BPM pedestal noise, PMT ADC noise, properly subtracting pedestals in the on-board FPGA, optimizing number of samples for baseline and peak, 119MHz to lock local ADC clocks, checkout of toroid sampling ADC, checkout of A-Line BPM processors, and sensitivity of BPM electronics to temperature.

## Appendix: Detailed Run-by-Run Results

The following tables contain the detailed run-by-run results for each measuring device for most of the above runs. They are included for reference.

Figures 2, 3, and 4 give the individual run results for the ASSET BPMS and toroids for the half-wave plate cancellation studies. Note, especially, the change with run number in the Y position differences for half-wave plate out. These runs were taken over a 12-hour period, and suggest that the systematics are not especially stable in the ASSET region. Can we correlate this with a drift in the injector systematics? Or is it more likely a drift in the beam tune downstream of the injector?

Table 15 contains SCP results for a couple other runs.

| Meas | 1026/7 | 1041 |
|---|---|---|
| TR488 (ppm) | -1.4 ± 27/1.2 | -8 ± 42/2.5 |
| TR560 (ppm) | -46 ± 27/1.2 | -30 ± 41/2.4 |
| X392 (nm) | | 240 ± 324/54 |
| Y392 (nm) | | 0 ± 204/34 |
| X402 (nm) | 4450 ± 112 | 1860 ± 179 |
| Y402 (nm) | -430 ± 109 | -1370 ± 349 |
| X405 (nm) | -1050 ± 252 | 1275 ± 474 |
| Y405 (nm) | -325 ± 286 | -1220 ± 546 |
| IA corr (ppm) | 298 ± 55 | 513 ± 90 |
| X corr (nm) | | -303 ± 198 |
| Y corr (nm) | | 4 ± 159 |
| # runs | ~505 | 36pos, 288 int |
| Notes | SCP IA FDBK<br>-2I, dCP=+400 | SCP IA, POS FDBK<br>-2I, dCP=+400 |

Table 15: SCP DAQ Results for other runs. Conditions as stated.

Figure 5 contains run-by-run results for the ASSET toroids from runs in which the Intensity Asymmetry feedback loop was under E158 DAQ control. The data is broken down by toroid asymmetry and by toroid asymmetry difference, as well as by timeslot for each toroid. One item to note is that there is a significant difference between the asymmetries on the two timeslots.

Figure 6 summarizes ASSET toroid results from a number of other runs. These include a second study of dependence on $\Delta$CP, a run with a short pulse (100ns vs. the normal 400ns), and several other miscellaneous runs. The data from these runs are included in table 2 as the line "Other Runs."

Figures 7 and 8 summarize results from the individual BPMs at ASSET for a number of different runs, including the Asymmetry Inverter runs, the study of long pulse vs. short pulse, the effect of beam tune on systematics, and the effect of choice of voltages on the Pockels cells. The meaningful data in these numbers is summarized in tables earlier in this paper.

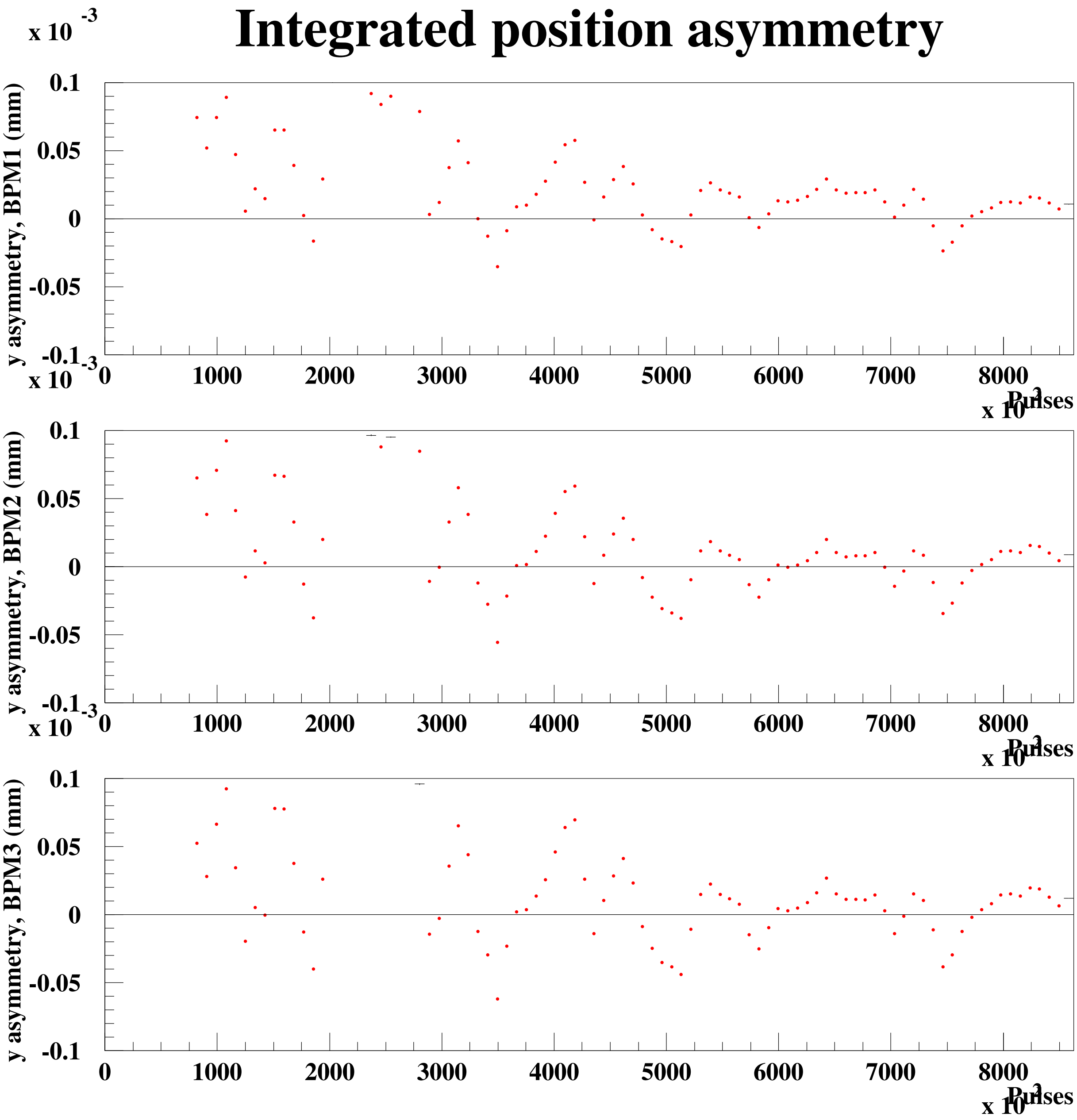


Figure 1: Integrated Y position differences as a function of time during an E158 position feedback run.

| Run # | HALF−WAVE IN | | | | | | | | | | | |
|---|---|---|---|---|---|---|---|---|---|---|---|---|
| | **toroid 1 asymmetry** | | | | **toroid 2 asymmetry** | | | | **A1−A2** | | | |
| | timeslot 1 | | timeslot 2 | | timeslot 1 | | timeslot 2 | | timeslot 1 | | timeslot 2 | |
| | mean (ppm) | error (ppm) | mean (ppm) | error (ppm) | mean (ppm) | error (ppm) | mean (ppm) | error (ppm) | mean (ppb) | error (ppb) | mean (ppb) | error (ppb) |
| 1007 | −2.71 | 13.83 | 4.39 | 13.31 | −2.48 | 13.83 | 4.34 | 13.32 | 94.95 | 77.28 | −43.67 | 75.14 |
| 1009 | −10.55 | 14.41 | 16.6 | 13.86 | −10.6 | 14.4 | 16.28 | 13.86 | −46.72 | 85.54 | 77.93 | 82.46 |
| 1014 | 7.08 | 17.91 | −10.6 | 17.89 | 7.73 | 17.91 | −10.42 | 17.89 | −90.09 | 71.76 | −138 | 71.76 |
| 1016 | −4.33 | 18.67 | 1.61 | 18.64 | −4.53 | 18.67 | 1.74 | 18.64 | −16.64 | 82.66 | −133.6 | 82.05 |
| 1018 | −22.74 | 19.05 | −8.13 | 19.06 | −23.14 | 19.04 | −7.98 | 19.06 | 10.06 | 93.27 | 37.65 | 93.16 |
| AVG | −6.28 | 7.29 | 3.07 | 7.14 | −6.22 | 7.29 | 3.05 | 7.14 | −12.19 | 36.28 | −49.32 | 35.76 |
| Timesl AVG | −1.5 | 5.1 | | | −1.49 | 5.1 | | | −31.03 | 25.47 | | |

| Run # | HALF−WAVE OUT | | | | | | | | | | | |
|---|---|---|---|---|---|---|---|---|---|---|---|---|
| | **toroid 1 asymmetry** | | | | **toroid 2 asymmetry** | | | | **A1−A2** | | | |
| | timeslot 1 | | timeslot 2 | | timeslot 1 | | timeslot 2 | | timeslot 1 | | timeslot 2 | |
| | mean (ppm) | error (ppm) | mean (ppm) | error (ppm) | mean (ppm) | error (ppm) | mean (ppm) | error (ppm) | mean (ppb) | error (ppb) | mean (ppb) | error (ppb) |
| 1005 | −0.81 | 13.11 | −24.03 | 12.63 | −1.12 | 13.11 | −23.95 | 12.63 | 44.46 | 75.49 | −40.62 | 72.93 |
| 1008 | −11.68 | 13.54 | −15.28 | 13.17 | −11.63 | 13.53 | −15.44 | 13.17 | −55.92 | 73.34 | −24.45 | 70.89 |
| 1013 | −10.05 | 17.17 | −9.45 | 17.12 | −10.32 | 17.18 | −9.87 | 17.12 | 70.15 | 71.7 | −89.57 | 72.01 |
| 1015 | −15.33 | 18.81 | −31.39 | 18.89 | −16.18 | 18.83 | −31.13 | 18.89 | 35.12 | 83.43 | −99.04 | 83.33 |
| 1017 | −10 | 15.26 | −23.67 | 15.24 | −9.48 | 15.27 | −23.84 | 15.25 | −85.62 | 72.35 | −27.17 | 71.87 |
| AVG | −8.67 | 6.78 | −20.43 | 6.66 | −8.78 | 6.78 | −20.52 | 6.66 | −0.29 | 33.51 | −53.73 | 33.02 |
| Timesl AVG | −14.65 | 4.75 | | | −14.75 | 4.75 | | | −27.41 | 23.52 | | |

Figure 2: E158 DAQ Toroid $\lambda/2$ Flip Data.

| Run # | **HALF−WAVE IN** | | | | | | | |
|---|---|---|---|---|---|---|---|---|
| | **x1 asymmetry** | | **x2 asymmetry** | | **x3 asymmetry** | | **X asymmetry diff** | |
| | mean | error | mean | error | mean | error | mean | error |
| 1007 | −5.96 | | | | | | | |
| 1009 | | | | | | | | |
| 1014 | 175 | 25 | 176 | 19 | 195 | 23 | −7.92 | 2.07 |
| 1016 | 120 | 27 | 80 | 21 | 55 | 21 | −0.13 | 2.61 |
| 1018 | 155 | 36 | 104 | 26 | 57 | 25 | 1.98 | 2.74 |
| AVG | 150.72 | 16.34 | 126.25 | 12.39 | 101.52 | 13.18 | −3.12 | 1.39 |

| Run # | **HALF−WAVE OUT** | | | | | | | |
|---|---|---|---|---|---|---|---|---|
| | **x1 asymmetry** | | **x2 asymmetry** | | **x3 asymmetry** | | **X asymmetry diff** | |
| | mean | error | mean | error | mean | error | mean | error |
| 1005 | | | | | | | | |
| 1008 | | | | | | | | |
| 1013 | 453 | 26 | 279 | 19 | 149 | 23 | −2.66 | 2.05 |
| 1015 | 70 | 27 | 3 | 21 | −66 | 22 | −7.82 | 2.6 |
| 1017 | 132 | 27 | 54 | 19 | −16 | 19 | −4.62 | 2.06 |
| AVG | 224.31 | 15.39 | 119.02 | 11.32 | 15.01 | 12.19 | −4.63 | 1.27 |

***Averaging Halfwave Plate Runs With / Without Sign Flip***

| | | | | | | | | |
|---|---|---|---|---|---|---|---|---|
| L/2 IN | 150.72 | 16.34 | 126.25 | 12.39 | 101.52 | 13.18 | −3.12 | 1.39 |
| L/2 OUT | 224.31 | 15.39 | 119.02 | 11.32 | 15.01 | 12.19 | −4.63 | 1.27 |
| AVG | 189.73 | 11.2 | 122.31 | 8.36 | 54.91 | 8.95 | −3.95 | 0.94 |
| AVG sign Flip | −48.08 | 11.2 | −7.43 | 8.36 | 38.73 | 8.95 | 1.12 | 0.94 |

Figure 3: E158 DAQ X Position Difference Data for $\lambda/2$ Flips.

| Run # | HALF−WAVE IN | | | | | | | |
|---|---|---|---|---|---|---|---|---|
| | **y1 asymmetry** | | **y2 asymmetry** | | **y3 asymmetry** | | **Y asymmetry diff** | |
| | mean | error | mean | error | mean | error | mean | error |
| 1007 | | | | | | | | |
| 1009 | | | | | | | | |
| 1014 | −1642 | 78 | −1605 | 76 | −1691 | 78 | 11.98 | 5.79 |
| 1016 | −1950 | 115 | −1886 | 108 | −1956 | 107 | 18.42 | 6.03 |
| 1018 | −1994 | 152 | −1904 | 139 | −2039 | 140 | 45.43 | 8.09 |
| AVG | −1778 | 59.42 | −1732.38 | 56.74 | −1826.11 | 57.47 | 21.45 | 3.71 |

| Run # | HALF−WAVE OUT | | | | | | | |
|---|---|---|---|---|---|---|---|---|
| | **y1 asymmetry** | | **y2 asymmetry** | | **y3 asymmetry** | | **Y asymmetry diff** | |
| | mean | error | mean | error | mean | error | mean | error |
| 1005 | | | | | | | | |
| 1008 | | | | | | | | |
| 1013 | −290 | 78 | −308 | 76 | −323 | 79 | 1.7 | 5.74 |
| 1015 | −731 | 109 | −686 | 100 | −764 | 100 | 19.95 | 6.4 |
| 1017 | −946 | 105 | −926 | 97 | −1003 | 98 | 9.53 | 5.48 |
| AVG | −574.81 | 54.29 | −580.74 | 51.34 | −638.36 | 52.39 | 9.72 | 3.37 |

***Averaging Halfwave Plate Runs With / Without Sign Flip***

| | | | | | | | | |
|---|---|---|---|---|---|---|---|---|
| L/2 IN | −1778 | 59.42 | −1732.38 | 56.74 | −1826.11 | 57.47 | 21.45 | 3.71 |
| L/2 OUT | −574.81 | 54.29 | −580.74 | 51.34 | −638.36 | 52.39 | 9.72 | 3.37 |
| AVG | −1122.31 | 40.08 | −1099.16 | 38.07 | −1177.37 | 38.72 | 15.03 | 2.49 |
| AVG sign Flip | −495.81 | 40.08 | −460.52 | 38.07 | −480.04 | 38.72 | 4.37 | 2.49 |

Figure 4: E158 DAQ X Position Difference Data for $\lambda/2$ Flips.

| **E158 FDBK Runs** | **Toroid 1** | | | | Toroid 2 | | | | Asym Diff | | | |
|---|---|---|---|---|---|---|---|---|---|---|---|---|
| | timeslot 1 | | timeslot 2 | | timeslot 1 | | timeslot 2 | | timeslot 1 | | timeslot 2 | |
| | mean (ppm) | error (ppm) | mean (ppm) | error (ppm) | mean (ppm) | error (ppm) | mean (ppm) | error (ppm) | mean (ppb) | error (ppb) | mean (ppb) | error (ppb) |
| 1040 | −12.26 | 11.42 | 12.26 | 11.39 | −12.18 | 11.4 | 11.93 | 11.38 | −44.03 | 50.93 | 141.7 | 50.84 |
| 1044 | −9.74 | 37.58 | −0.03 | 37.22 | −9.36 | 37.53 | −0.14 | 37.17 | −70.6 | 148.72 | 7.2 | 148.51 |
| 1047 | −29.66 | 58.92 | 56.9 | 58.66 | −30.19 | 58.84 | 57.86 | 58.61 | 257.2 | 263.25 | 34.31 | 265.11 |
| 1049 | −5.33 | 14.69 | 4.9 | 14.64 | −5.39 | 14.67 | 4.89 | 14.62 | −50.91 | 63.2 | 49.87 | 63.18 |
| 1052 | 0.5 | 20.82 | 2.68 | 20.84 | 0.29 | 20.8 | 2.97 | 20.81 | −13.4 | 75.94 | −76.96 | 75.65 |
| AVG | −8.52 | 8 | 8.93 | 7.98 | −8.53 | 7.99 | 8.81 | 7.97 | −36.28 | 33.92 | 62.73 | 33.87 |
| Timeslot AVG | 0.22 | 5.65 | | | 0.16 | 5.65 | | | 13.31 | 23.97 | | |

Figure 5: E158 DAQ Intensity Asymmetry Feedback Runs: Toroid Data. Asymmetries listed for toroids T1 and T2 at ASSET, as well as the pairwise difference in asymmetry between T1 and T2.

| **Special Runs** | Toroid 1 Asymmetry | | | | Toroid 2 Asymmetry | | | | Asym Diff (A1 − A2) | | | |
|---|---|---|---|---|---|---|---|---|---|---|---|---|
| | timeslot 1 | | timeslot 2 | | timeslot 1 | | timeslot 2 | | timeslot 1 | | timeslot 2 | |
| | mean (ppm) | error (ppm) | mean (ppm) | error (ppm) | mean (ppm) | error (ppm) | mean (ppm) | error (ppm) | mean (ppb) | error (ppb) | mean (ppb) | error (ppb) |
| DCP −400V | 28.5 | 21.77 | −33.51 | 21.91 | 28.49 | 21.78 | −33.12 | 21.92 | 35.12 | 102.53 | −137.1 | 101.99 |
| DCP 0V | 21.11 | 24.16 | −56.51 | 24.25 | 21.84 | 24.18 | −56.59 | 24.27 | −2.18 | 117.69 | 166.9 | 117.69 |
| DCP +400V | −38 | 10.64 | −27.35 | 10.63 | −37.97 | 10.64 | −27.03 | 10.63 | −48.62 | 45.46 | −57.37 | 45.57 |
| 100ns pulse | −12.89 | 31.89 | −26.32 | 31.9 | −12.35 | 31.91 | −25.18 | 31.92 | −445.1 | 295.8 | −401.6 | 296.97 |
| 1041 | −28.82 | 25.37 | −29.27 | 25.3 | −29.03 | 25.35 | −28.93 | 25.28 | 89.33 | 100.23 | −2.35 | 100.02 |
| 1033 | −14.63 | 38.23 | −12.04 | 37.78 | −14.49 | 38.19 | −11.09 | 37.74 | 38.97 | 159.07 | −208.9 | 159.62 |
| 1035 | 0.03 | 24.41 | 3.84 | 24.25 | 0.2 | 24.39 | 3.62 | 24.22 | 98.62 | 101.93 | −136.6 | 102.36 |
| 1045 & 1046 | −41.15 | 37.12 | 11.83 | 37.35 | −41.28 | 37.07 | 12.03 | 37.29 | 47.62 | 154.79 | −96.32 | 155.43 |
| AVG | −18.42 | 7.39 | −25.85 | 7.39 | −18.32 | 7.4 | −25.53 | 7.39 | −3.74 | 32.62 | −62.7 | 32.66 |
| Timeslot AVG | −22.14 | 5.23 | | | −21.92 | 5.23 | | | −33.19 | 23.08 | | |

Figure 6: Other E158 DAQ Toroid Data.

| Run # | Asym Inv +−2I, E158 IA, POS fdbks | | | | | | | | | | |
|---|---|---|---|---|---|---|---|---|---|---|---|
| | **x1 asymmetry** | | | **x2 asymmetry** | | | **x3 asymmetry** | | | **X asymmetry diff** | |
| | mean | error | 1/N error | mean | error | 1/N error | mean | error | 1/N error | mean | error |
| 1049 (−2I) | −14 | 75 | 11.2 | −18 | 50 | 7.5 | −27 | 35 | 5.2 | −1.2 | 3.1 |
| 1052 (+2I) | −24 | 84 | 15.6 | 9 | 54 | 10 | 26 | 38 | 7 | −8.2 | 4.3 |
| ave sqrtN | −18.44 | 55.95 | | −5.54 | 36.69 | | −2.67 | 25.74 | | −3.59 | 2.51 |
| ave 1/N | −17.4 | 9.1 | | −8.28 | 6 | | −8.15 | 4.17 | | | |

| Run # | Long Pulse vs. Short Pulse | | | | | | | | | | |
|---|---|---|---|---|---|---|---|---|---|---|---|
| | **x1 asymmetry** | | | **x2 asymmetry** | | | **x3 asymmetry** | | | **X asymmetry diff** | |
| | mean | error | 1/N error | mean | error | 1/N error | mean | error | 1/N error | mean | error |
| 400ns | −108 | 13 | | −144 | 11 | | −188 | 10 | | −2.15 | 1.18 |
| 75ns, <0.8 | −201 | 39 | | −260 | 37 | | −328 | 41 | | −9.48 | 8.12 |
| 75ns, <0.5 | −201 | 39 | | −260 | 37 | | −328 | 41 | | | |

| Run # | Effect of Beam Tune | | | | | | | | | | |
|---|---|---|---|---|---|---|---|---|---|---|---|
| | **x1 asymmetry** | | | **x2 asymmetry** | | | **x3 asymmetry** | | | **X asymmetry diff** | |
| | mean | error | 1/N error | mean | error | 1/N error | mean | error | 1/N error | mean | error |
| DCP +400 | −108 | 13 | | −144 | 11 | | −188 | 10 | | −2.15 | 1.18 |
| 1035 | 25 | 43 | | 25 | 36 | | 29 | 30 | | −0.17 | 7.12 |
| 1040 | −331 | 35 | | −291 | 25 | | −268 | 20 | | 1.52 | 3.07 |

| Run # | Effect of Pockels Cell Voltages | | | | | | | | | | |
|---|---|---|---|---|---|---|---|---|---|---|---|
| | **x1 asymmetry** | | | **x2 asymmetry** | | | **x3 asymmetry** | | | **X asymmetry diff** | |
| | mean | error | 1/N error | mean | error | 1/N error | mean | error | 1/N error | mean | error |
| DCP −400 | −141 | 32 | | −177 | 24 | | −206 | 21 | | −1.63 | 12.71 |
| DCP 0 | −120 | 38 | | −137 | 29 | | −174 | 24 | | 1.39 | 5.91 |
| DCP +400 | −108 | 13 | | −144 | 11 | | −188 | 10 | | −2.15 | 1.18 |

Figure 7: Other E158 DAQ X Position Difference Results.

| Run # | Asym Inv +−2I, E158 IA, POS fdbks | | | | | | | | | | |
|---|---|---|---|---|---|---|---|---|---|---|---|
| | **y1 asymmetry** | | | **y2 asymmetry** | | | **y3 asymmetry** | | | **Y asymmetry diff** | |
| | mean | error | 1/N error | mean | error | 1/N error | mean | error | 1/N error | mean | error |
| 1049 (−2I) | −1 | 52 | 7.8 | −9 | 64 | 9.6 | −25 | 73 | 10.9 | −4.5 | 3.1 |
| 1052 (+2I) | −30 | 62 | 11.5 | −33 | 76 | 14.1 | −51 | 87 | 16.1 | −3 | 4.3 |
| ave sqrtN | −12.98 | 39.84 | | −18.96 | 48.95 | | −35.74 | 55.92 | | −3.99 | 2.51 |
| ave 1/N | −10.14 | 6.46 | | −16.6 | 7.94 | | −33.17 | 9.03 | | | |

| Run # | Long Pulse vs. Short Pulse | | | | | | | | | | |
|---|---|---|---|---|---|---|---|---|---|---|---|
| | **y1 asymmetry** | | | **y2 asymmetry** | | | **y3 asymmetry** | | | **Y asymmetry diff** | |
| | mean | error | 1/N error | mean | error | 1/N error | mean | error | 1/N error | mean | error |
| 400ns | −264 | 61 | | −315 | 54 | | −362 | 62 | | −3.94 | 4.97 |
| 75ns, <0.8 | 578 | 128 | | 554 | 126 | | 461 | 142 | | 48.6 | 32.21 |
| 75ns, <0.5 | 401 | 302 | | 621 | 305 | | 593 | 406 | | | |

| Run # | Effect of Beam Tune | | | | | | | | | | |
|---|---|---|---|---|---|---|---|---|---|---|---|
| | **y1 asymmetry** | | | **y2 asymmetry** | | | **y3 asymmetry** | | | **Y asymmetry diff** | |
| | mean | error | 1/N error | mean | error | 1/N error | mean | error | 1/N error | mean | error |
| DCP +400 | −264 | 61 | | −315 | 54 | | −362 | 62 | | −3.94 | 4.97 |
| 1035 | 33 | 104 | | 30 | 124 | | 40 | 138 | | −0.42 | 9.15 |
| 1040 | 737 | 43 | | 853 | 60 | | 909 | 54 | | 54.47 | 5.51 |

| Run # | Effect of Pockels Cell Voltages | | | | | | | | | | |
|---|---|---|---|---|---|---|---|---|---|---|---|
| | **y1 asymmetry** | | | **y2 asymmetry** | | | **y3 asymmetry** | | | **Y asymmetry diff** | |
| | mean | error | 1/N error | mean | error | 1/N error | mean | error | 1/N error | mean | error |
| DCP −400 | −1236 | 171 | | −1209 | 152 | | −1272 | 165 | | 41.83 | 12.35 |
| DCP 0 | −951 | 187 | | −907 | 166 | | −1027 | 178 | | 51.39 | 13.55 |
| DCP +400 | −264 | 61 | | −315 | 54 | | −362 | 62 | | −3.94 | 4.97 |

Figure 8: Other E158 DAQ Y Position Difference Results.